Asian Journal of Chemistry; Vol. 38, No. 1 (2026), 164-172
ASIAN JOURNAL OF CHEMISTRY
https://doi.org/10.14233/ajchem.2026.34961

Design, Synthesis, *in silico* Analysis and Pharmacological Evaluation of Coumarin Derived Mercaptotriazole Derivatives as MCL-1 Inhibitors

G. BUELA PRIYANKA[1], SHAIK HARUN RASHEED[1,*], RAJALA SRIKALA[1], K. VENKATA SWATHI KRISHNA[2], Y. PRAPURNA CHANDRA[3], G. RAJESWARI[4], P. VENU GOPALAIAH[3] and KOMMU PRADEEP[5]

[1]School of Pharmacy, Guru Nanak Institutions Technical Campus (Autonomous), Ibrahimpatnam-501506, India
[2]Department of Pharmaceutics, Swathi College of Pharmacy, Venkatachalam, SPSR Nellore-524320, India
[3]Department of Pharmacology, Ratnam Institute of Pharmacy, Pidathapolur, Nellore-524411, India
[4]Department of Pharmacology, Sastra College of Pharmacy, Nellore-524311, India
[5]Faculty of Health Sciences, Villa College, Kaafu Atoll, Male-2002, Maldives

*Corresponding author: E-mail: shaikharunrasheed@gmail.com

Received: 25 September 2025 *Accepted*: 18 November 2025 *Published online*: 31 December 2025 AJC-22234

Design and synthesis of new series of 4-amino-5-mercapto-4*H*-1,2,4-triazoles connected to coumarin ring and assessed for cytotoxity and the study of docking studies was done against MDA-MB-231 cell lines. Using substituted diols, a series of new coumarin linked 4-amino-5-mercapto-4*H*-1,2,4-triazoles derivatives were synthesized from substituted diols. Moreover, the elucidation of the newly synthesized mercaptotriazole derivatives was achieved by spectral data. An MTT assay was employed to evaluate the antineoplastic activity against triple-negative breast cancer (TNBC) and the synthesized compounds demonstrated promising, potent, and innovative inhibitory effects, highlighting their potential for the development of new anticancer therapies. Compounds **8h**, **8d**, **8e**, **8b**, **8i**, **8j** and **8a** exhibit high binding energies with target receptor MCL-1 enzyme of the MDA-MB231 cells, where remaining compounds exhibit good binding interactions with target protein. *In silico* Docking studies verified the uncompetitive inhibition of MCL-1 enzyme.

Keywords: Coumarins, Mercaptotriazole, Chromen-2-one derivatives, MCL-1 enzyme, Antineoplastic activity, *In silico* studies.

INTRODUCTION

Breast cancer is one of the leading causes of cancer-related morbidity and mortality among women worldwide. Neoplasia, characterized by the uncontrolled proliferation of cells, underlies the development of breast cancer and arises primarily from genetic mutations in normal breast epithelial cells [1]. If cancerous cells are undetected early, they may spread to other organs and invade the nearby tissues, increasing the risk of mortality and complicating the treatment procedure. By raising the chance of a successful therapy course and breast-conserving surgery, early identification of the breast cancer significantly improves the long-term outcomes [2]. Despite their widespread usage, traditional screening methods and the clinical breast examinations have their limitations and the decreased sensitivity. The risk of breast cancer was identified by risk assessment techniques and patients who are at high risk might benefit from taking the drugs that lowers risk [3]. Menopausal state influences the choice for medication. Genetic and the inherited predisposition were among the risk factors related to breast cancer. Locoregional therapy is the cornerstone of breast cancer treatment and is considered curative when the disease is diagnosed at an early stage. If necessary, systemic therapy might be given either prior the surgery [4].

Mercaptotriazole derivatives are well-known chemical scaffolds exhibiting diverse biological activities, including antimicrobial, antibacterial and antifungal effects [5-8]. Beyond these properties, they serve as versatile intermediates in the synthesis of various heterocyclic drugs with significant physiological activity [9,10]. Leveraging these features, novel compounds are designed by integrating triazole and coumarin pharmacophores into a single molecular framework. Such hybridization is anticipated to enhance pharmacological efficacy, potentially offering new avenues for anticancer drug development. In this study, we explored the binding potential of the designed

triazole-coumarin hybrids against MCL-1 using molecular docking with the crystal structure (PDB ID: 3WIX) [11], aiming to identify promising candidates for triple-negative breast cancer (TNBC) therapy.

EXPERIMENTAL

Analytical grade of 98% pure chemicals and solvents were brought from Sigma-Aldrich and used without further purification. Thin-layer chromatography (TLC) plates were prepared using 0.5 mm thick aluminum sheets (Merck) pre-coated with silica gel 60 F_{254} sheets. To record an infrared (IR) spectra, KBr pellet method was used using an FTIR spectrometer (model: Thermo-Scientific Nicolet iS5/iS10). ^{1}H NMR spectra was obtained using a VARIAN NMR spectrometer operating at 500 MHz. The melting points of the synthesized compounds were determined using a Remi electronic melting point apparatus and are uncorrected.

General procedure

Synthesis of 4-amino-5-mercapto-4*H*-1,2,4-triazole-2*H*-chromen-2-one derivatives (8a-j): The titled mercapto-triazole derivatives were synthesized *via* a modified literature procedure [12]. Substituted diols were reacted with ethyl aceto-acetate at 70-80 ºC for 30 min using Eaton's reagent as catalyst to form coumarin derivatives. These intermediates were treated with ethyl bromoacetate in DMF with K_2CO_3 at 25 ºC for 8 h, followed by sequential reactions with hydrazine hydrate, CS_2 in the presence of KOH, and a final hydrazine hydrate reflux to yield the target compounds (**Scheme-I**). The products were purified by recrystallization from alcohol.

5-((4-Amino-5-mercapto-4*H*-1,2,4-triazole-3-yl)methoxy-8-ethyl-4-methyl-2*H*-chromen-2-one (8a): White solid, yield: 88%, m.p.: 256-268 ºC; ^{1}H NMR (500 MHz, $CHCl_3$-d_6, δ ppm): 1.08 (t, 3H), 1.36 (s, 2H), 1.58 (2H), 2.45-2.55 (s, 3H), 5.33 (s, 2H), 6.22 (s, 1H), 7.10 (s, 1H), 7.38 (s, 1H), 13.73 (s, H); ^{13}C NMR (125 MHz, $CHCl_3$-d_6, δ ppm): 14.1, 22.3, 23.8, 31.0, 66.9, 112.3, 113.1, 124.8, 128.7, 150.5, 151.8, 155.9, 160.8, 166.9, 188.75; HRMS: *m/z* for $C_{17}H_{20}N_4O_3S$ ([M+H]$^+$): 360.13; found 360.43.

5-((4-Amino-5-mercapto-4*H*-1,2,4-triazole-3-yl)methoxy-8-hexyl-4-methyl-2*H*-chromen-2-one (8b): White solid, yield: 73%, m.p.: 280-295 ºC; ^{1}H NMR (500 MHz, $CHCl_3$-d_6, δ ppm): 1.08 (t, 3H), 1.36 (s, 2H), 1.58 (2H), 2.45-2.55 (s, 3H), 5.33 (s, 2H), 6.22 (s, 1H), 7.10 (s, 1H), 7.38 (s, 1H), 13.74 (s, H); ^{13}C NMR (125 MHz, $CHCl_3$-d_6, δ ppm): 14.1, 22.7, 23.8, 31.3, 31.3, 31.9,66.9, 112.3, 112.7, 113.5, 124.8, 128.9, 150.8, 151.9, 152.3, 160.9, 166.7; HRMS: *m/z* for $C_{19}H_{24}N_4O_3S$ ([M+H]$^+$): 388.16, found 388.26.

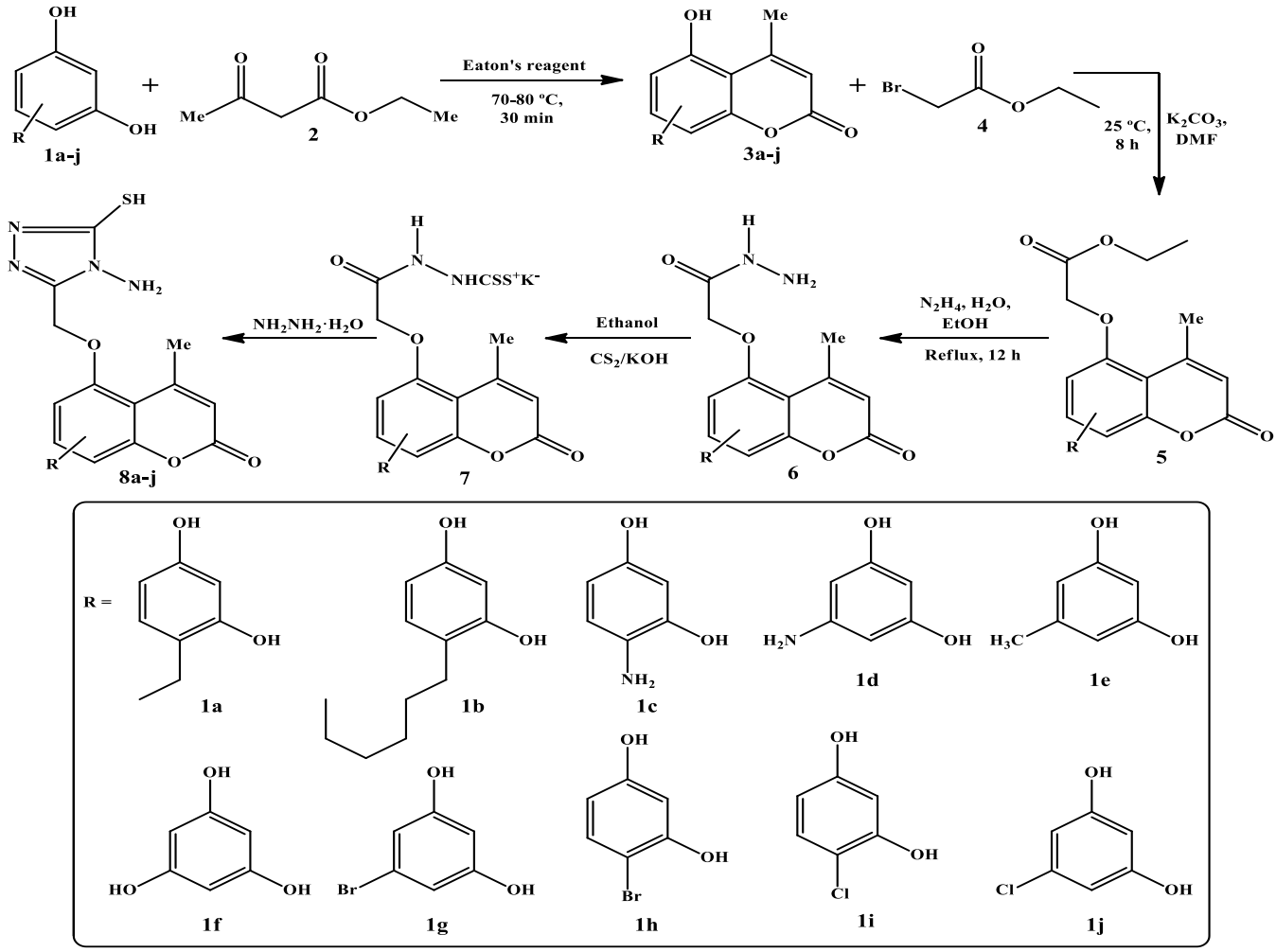

Scheme-I: Synthesis of 5-((4-amino-5-mercapto-4*H*-1,2,4-triazole-3-yl)methoxy-8-ethyl-4-methyl-2*H*-chromen-2-one derivatives

Synthesis of 8-amino-5-((4-amino-5-mercapto-4*H*-1,2,4-triazole-3-yl)methoxy)-4-methyl-2*H*-chromen-2-one (8c): White solid, yield: 75%, m.p.: 268-288 ºC, ^{1}H NMR (500 MHz, $CHCl_3$-d_6, δ ppm): 2.45-2.55 (t, 3H), 5.23 (s, 2H), 5.32 (s, 2H), 5.670 (s, 2H), 6.28 (s, 1H), 6.85 (s, 1H), 13.93 (s, 1H). ^{13}C NMR (125 MHz, $CHCl_3$-d_6, δ ppm): 23.3, 66.9, 112.3, 113.1, 114. 8, 116.7, 135.5, 138.8, 138.9, 148.8, 151.9, 155.5, 160.7, 166.7; HRMS: *m/z* for $C_{13}H_{13}N_5O_3S$ ($[M+H]^+$): 319.07, found 319.34.

7-Amino-5-((4-amino-5-mercapto-4*H*-1,2,4-triazole-3-yl)methoxy)-4-methyl-2*H*-chromen-2-one (8d): White solid, yield: 62%, m.p.: 220-240 ºC; ^{1}H NMR (500 MHz, $CHCl_3$-d_6, δ ppm): 2.45 (t, 3 H), 5.23 (s, 2H), 5.32 (s, 2H), 5.60 (s, 2H), 6.18 (s, 1H), 6.20 (1 H), 6.28 (1H), 13.79 (s, 1H); ^{13}C NMR (125 MHz, $CHCl_3$-d_6, δ ppm): 23.8, 66.9, 92.8, 96.1, 109.8, 112.7, 150.1, 151.8, 155.5, 158.8, 160.8, 166.9; HRMS: *m/z* for $C_{13}H_{13}N_5O_3S$ ($[M+H]^+$): 319.07, found 319.07.

5-((4-Amino-5-mercapto-4*H*-1,2,4-triazole-3-yl)methoxy)-4,7-dimethyl-2*H*-chromen-2-one (3e): White solid, yield: 65%, m.p.: 260-270 ºC; ^{1}H NMR (500 MHz, $CHCl_3$-d_6, δ ppm): ^{1}H NMR (500 MHz, $CHCl_3$-d_6, δ ppm): 2.45 (t, 3H), 2.45 (s, 1H) 5.33 (s, 2H), 5.66 (2H), 6.22 (s, 1 H), 6.76 (s, 1H), 13.79 (s, 1H); ^{13}C NMR (125 MHz, $CHCl_3$-d_6, δ ppm): 21.3, 23.8, 31.0, 66.9, 109.8, 112.5, 113.8, 116.7, 140.5, 151.2, 151.7, 155.9, 157.8, 160.8, 166.9; HRMS: *m/z* for $C_{14}H_{14}N_4O_3S$ ($[M+H]^+$): 318.08, found 318.08.

5-((4-Amino-5-mercapto-4*H*-1,2,4-triazole-3-yl)methoxy)-7-hydroxy-4-methyl-2*H*-chromen-2-one (8f): White solid, yield: 76%, m.p.: 242-255 ºC; ^{1}H NMR (500 MHz, $CHCl_3$-d_6, δ ppm): 2.46 (t, 3H), 5.33 (s, 2H), 5.62 (s, 2H), 6.207 (s, 2H), 6.35 (s, 1H), 6.47 (1 H),10.29 (1H), 13.23 (s, 1H); ^{13}C NMR (125 MHz, $CHCl_3$-d_6, δ ppm): 23.8, 66.9, 92.3, 98.1, 112.8, 151.5, 154.8, 155.7,155.9, 159.4, 160.8, 166.9; HRMS: *m/z* for $C_{13}H_{12}N_4O_4S$ ($[M+H]^+$): 320.06, found 320.16.

5-((4-Amino-5-mercapto-4*H*-1,2,4-triazole-3-yl)methoxy)-7-bromo-4-methyl-2*H*-chromen-2-one (8g): White solid, yield: 85%, m.p.: 236-245 ºC; ^{1}H NMR (500 MHz, $CHCl_3$-d_6, δ ppm): 2.45 (t, 3H), 5.33 (s, 2H), 5.65 (s, 2H), 7.30 (s, 1H), 7.43 (s, 1H), 13.73 (s, 1H); ^{13}C NMR (125 MHz, $CHCl_3$-d_6, δ ppm): 23.8, 66.9, 112.3, 112.5, 114.3, 118.1, 151.5, 153.8, 155.9, 160.2, 166.6,166.8; HRMS: *m/z* for $C_{13}H_{11}BrN_4O_3S$ ($[M+H]^+$): 381.97, found 383.22.

5-((4-Amino-5-mercapto-4*H*-1,2,4-triazole-3-yl)methoxy)-8-bromo-4-methyl-2*H*-chromen-2-one (8h): White solid, yield: 75%, m.p.: 254-265 ºC; ^{1}H NMR (500 MHz, $CHCl_3$-d_6, δ ppm): 2.45 (t, 3H), 5.33 (s, 2H), 5.67 (s, 2H), 6.20 (s, 1H), 6.89 (s, 1H), 7.62 (1H), 13.73 (s, 1H); ^{13}C NMR (125 MHz, $CHCl_3$-d_6, δ ppm): 23.8,109.9, 111.3, 112.5, 114.8, 130.6, 147.5, 151.8, 155.9, 157.0, 160.8, 166.9; HRMS: *m/z* for $C_{13}H_{11}BrN_4O_3S$ ($[M+H]^+$): 383.97, found 383.22.

5-((4-Amino-5-mercapto-4*H*-1,2,4-triazole-3-yl)methoxy)-8-chloro-4-methyl-2*H*-chromen-2-one (8i): White solid, yield: 72%, m.p.: 291-294 ºC; ^{1}H NMR (500 MHz, $CHCl_3$-d_6, δ ppm): 2.46 (t, 3H), 5.33 (s, 2H), 5.67 (s, 2H), 6.27 (s, 1H), 6.98 (s, 1H), 7.48(1H), 13.73 (s, 1H); ^{13}C NMR (125 MHz, $CHCl_3$-d_6, δ ppm): 23.8, 66.9, 112.3, 112.5, 113.8, 122.2, 129.7, 146.5, 151.8, 155.9,156.2, 160.8, 166.9; HRMS: *m/z* for $C_{13}H_{11}ClN_4O_3S$ ($[M+H]^+$): 338.02, found 338.77.

5-((4-Amino-5-mercapto-4*H*-1,2,4-triazole-3-yl)methoxy)-7-chloro-4-methyl-2*H*-chromen-2-one (8j): White solid, yield: 76%, m.p.: 291-294 ºC; ^{1}H NMR (500 MHz, $CHCl_3$-d_6, δ ppm): 2.43 (t, 3H), 5.33 (s, 2H), 5.67 (s, 2H), 6.20 (s, 1H), 6.85 (s, 1H), 6.89 (1H), 13.73 (s, 1H). ^{13}C NMR (125 MHz, $CHCl_3$-d_6, δ ppm): 23.8, 66.9, 111.9, 112.1, 113.8, 116.6, 117.7, 134.5, 151.8, 152.9, 155.8, 159.4, 160.9; HRMS: *m/z* for $C_{13}H_{11}Cl_2N_4O_3S$ ($[M+H]^+$): 338.02, found 338.77.

Molecular docking: Docking studies were performed to identify potent breast cancer drugs by observing the molecular binding affinities of designed structures with MCL-1 receptor protein. The selection of the target receptor for docking is based on several factors such as resolution below 2.0 Å, the structure should be elucidated by X-ray diffraction techniques, consists of co-crystallized ligand and it does not have any breaks in the particular 3D structure of the protein.

MCL-1 target enzyme is the recently exploring target for identification of breast cancer agents comprising a bis-chalcone nucleus. The crystalline structure of the MCL-1 target receptor protein was obtained from protein databank which is having the resolution of 1.9 Å with PDB ID: 3WIX [11]. AutoDock 4.2.6 software was used to know the interactions of the designed 3D-structured mercaptotriazoles with the active site of 3WIX [13]. ChemSketch, version 2022.1.2, ACD/ Labs software used to design the structures and then converted into respective 3D design. By applying molecular mechanics they underwent energy minimizations required for the molecular docking and for preparing of corresponding pdb files. Using default parameters Grid-based docking studies was carried by and docking studies were performed by considering 7-(4-carboxyphenyl)-3-[3-(naphthalen-1-yloxy)-propyl]pyrazolo[1,5-*a*]pyridine-2-carboxylic acid as reference ligand at MCL-1 active site. Discovery Studio visualizers v21.1 is used to check the 2D and 3D binding interactions of ligands with receptor protein [14].

Anticancer activity: MDA-MB-231 human breast cancer epithelial cells were cultured in Dulbecco's Modified Eagle Medium (DMEM) or RPMI-1640, supplemented with 10% FBS and 1% penicillin–streptomycin and maintained at 37 ºC in a humidified atmosphere containing 5% CO_2. Cells were seeded into 96-well plates at a density of 5,000-10,000 cells per well in 100 μL of complete medium and allowed to adhere for 24 h. The cells were then treated with varying concentrations of the test compounds and incubated for 24, 48 and 72 h. Etoposide was used as a positive control, while the vehicle served as a negative control.

RESULTS AND DISCUSSION

Novel coumarin based mercaptotriazole derivatives (**8a-j**) were synthesized using various aromatic aldehydes following the outlined procedures and then characterized by the spectroscopic methods were evaluated for the anticancer activity against the cell lines MDA-MB-231. Molecular docking studies at the MCL1 target protein active site region gives data of the binding energies (kcal/moL), hydrogen bond length, number of the hydrogen bonds and the interacted amino acid residues, shown in Table-1.

TABLE-1
BINDING ENERGIES, H-BOND INTERACTIONS, AMINOACID RESIDUES,
HYDROGEN BOND LENGTHS PROFILES OF SYNTHESIZED COMPOUNDS **8a-j**

Compound	Binding energies (kcal/mol)	H-bond interactions (Å)	Amino acid residues	Hydrogen bond length (Å)
8a	-9.82	1	LEU267	4.32
8b	-9.88	1	LEU267	4.53
8c	-9.62	2	ARG263, LEU267	2.94, 4.90
8d	-9.92	0	No	–
8e	-9.92	2	ARG263, LEU267	4.84, 3.88
8f	-9.77	1	LEU267	4.69
8g	-9.60	1	LEU267	4.05
8h	-10.21	2	ARG263, LEU267	3.13, 4.96
8i	-9.88	3	ARG263, LEU267	3.33, 4.31, 4.17
8j	-9.85	1	ARG263	4.07
Reference	-12.25	1	ARG263	2.70

In comparison to the reference ligand, 7-(4-carboxyphenyl)-3-[3-(naphthalen-1-yloxy)propyl]pyrazolo[1,5-*a*]pyridine-2-carboxylic acid, which exhibited a binding energy of -12.27 kcal/mol, the synthesized compounds demonstrated strong and comparable binding affinities toward the MCL-1 receptor protein (PDB ID: 3WIX). Among the series, compound **8h** showed the highest binding affinity with a docking score of -10.21 kcal/mol, indicating the most favourable interaction with the active site of MCL-1.

Fig. 1 illustrates the 2D and 3D structures of the MCL-1 receptor and the binding modes of the reference ligand and compounds **8a-j** within the active site. Compound **8h** emer-

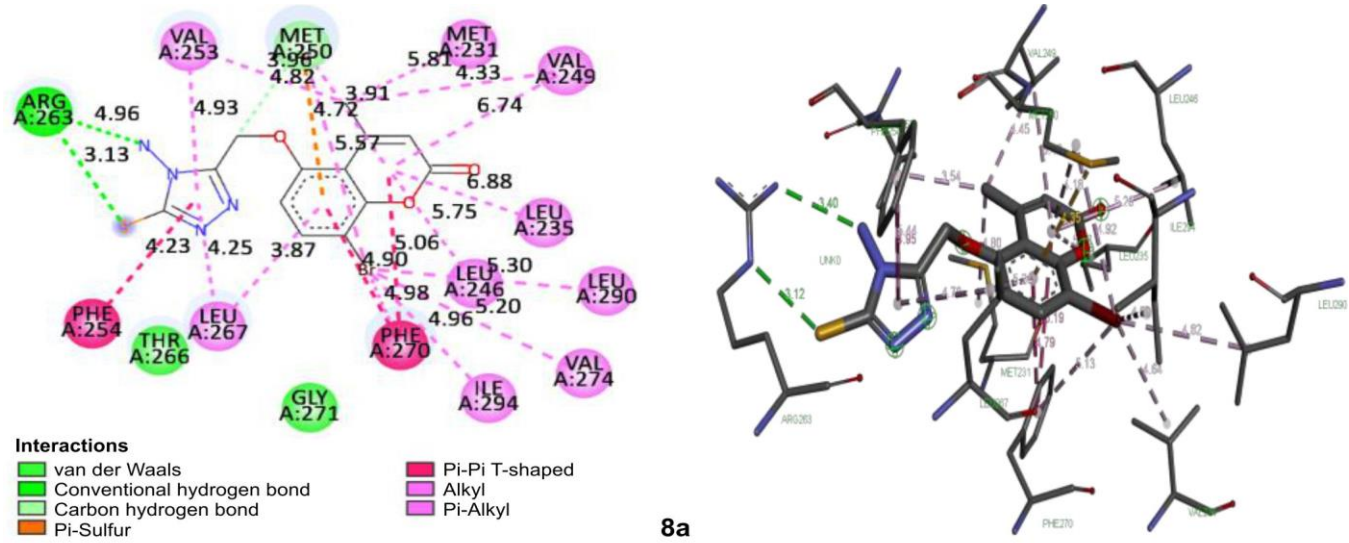

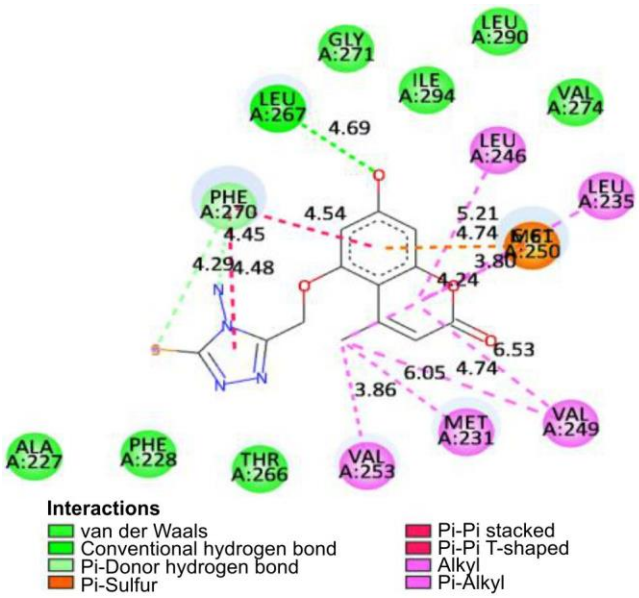
GLY A:271
LEU A:290
ILE A:294
LEU A:267
VAL A:274
LEU A:246
LEU A:235
PHE A:270
MET A:250
ALA A:227
PHE A:228
THR A:266
VAL A:253
MET A:231
VAL A:249
Interactions
van der Waals
Conventional hydrogen bond
Pi-Donor hydrogen bond
Pi-Sulfur
Pi-Pi stacked
Pi-Pi T-shaped
Alkyl
Pi-Alkyl

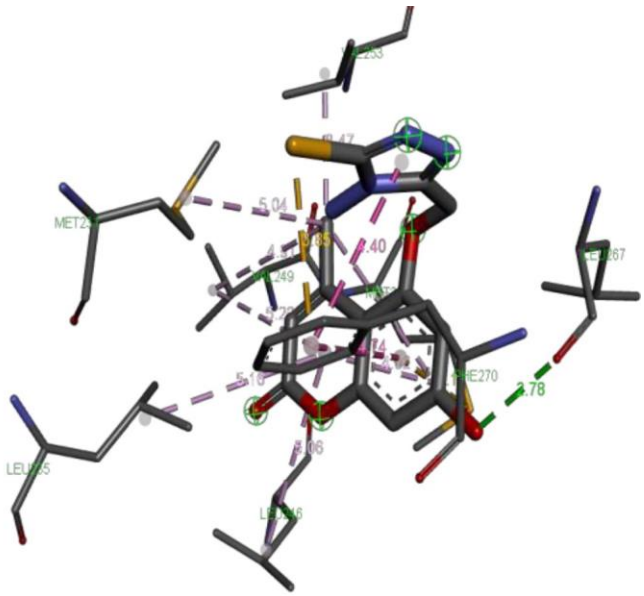

8c

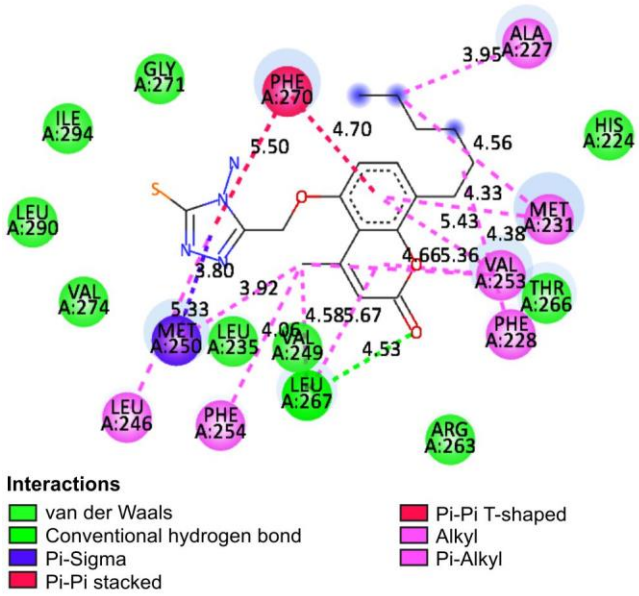
ALA A:227
GLY A:271
PHE A:270
ILE A:294
HIS A:224
LEU A:290
MET A:231
VAL A:274
VAL A:253
THR A:266
MET A:250
LEU A:235
PHE A:228
LEU A:246
PHE A:254
ARG A:263
Interactions
van der Waals
Conventional hydrogen bond
Pi-Sigma
Pi-Pi stacked
Pi-Pi T-shaped
Alkyl
Pi-Alkyl

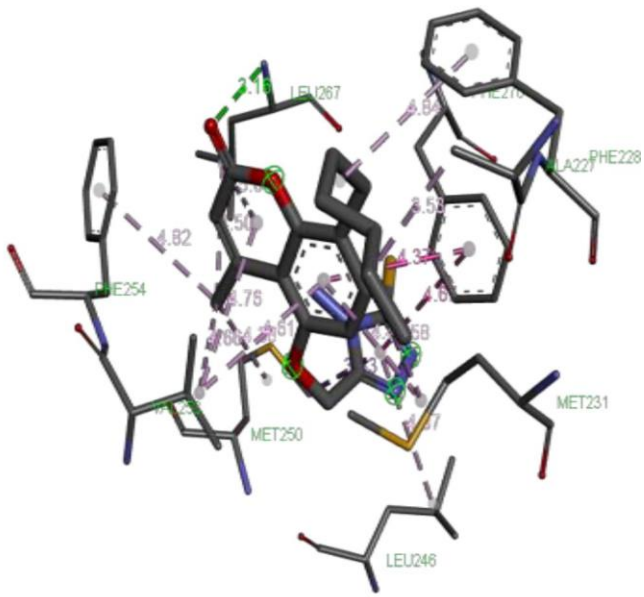

8d

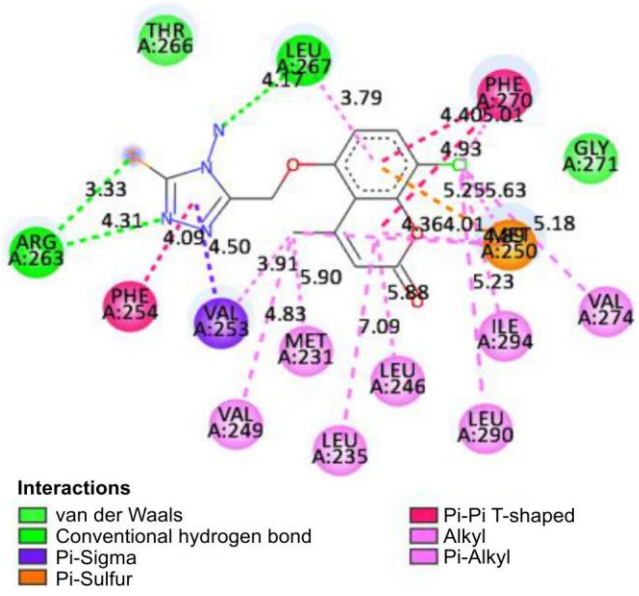
THR A:266
LEU A:267
PHE A:270
GLY A:271
ARG A:263
MET A:250
PHE A:254
VAL A:253
VAL A:274
MET A:231
ILE A:294
LEU A:246
VAL A:249
LEU A:235
LEU A:290
Interactions
van der Waals
Conventional hydrogen bond
Pi-Sigma
Pi-Sulfur
Pi-Pi T-shaped
Alkyl
Pi-Alkyl

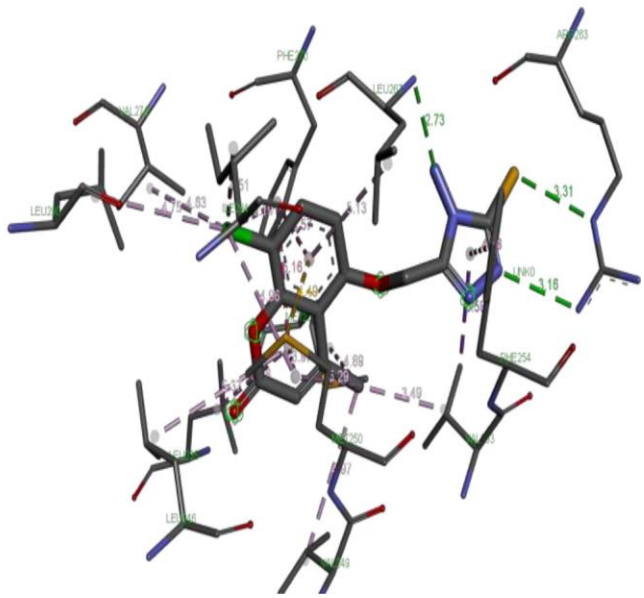

8e

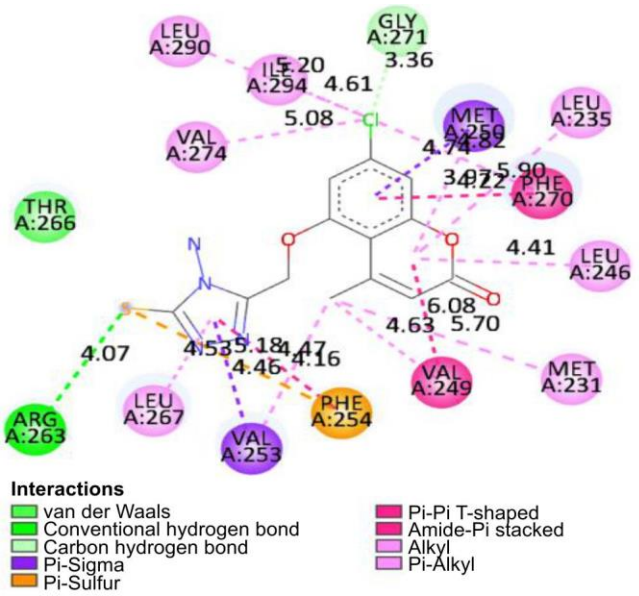
LEU A:290
GLY A:271
3.36
ILE A:294
4.61
5.20
5.08
Cl
MET A:250
LEU A:235
VAL A:274
4.74
4.82
3.77
5.90
3.22
PHE A:270
THR A:266
4.41
LEU A:246
6.08
4.63
5.70
4.07
4.53
5.18
4.47
4.46
4.16
VAL A:249
MET A:231
LEU A:267
PHE A:254
ARG A:263
VAL A:253
Interactions
van der Waals
Conventional hydrogen bond
Carbon hydrogen bond
Pi-Sigma
Pi-Sulfur
Pi-Pi T-shaped
Amide-Pi stacked
Alkyl
Pi-Alkyl

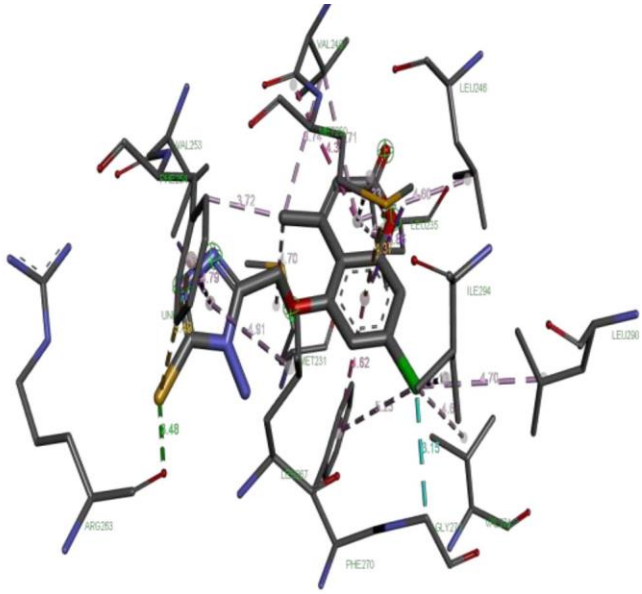

8f

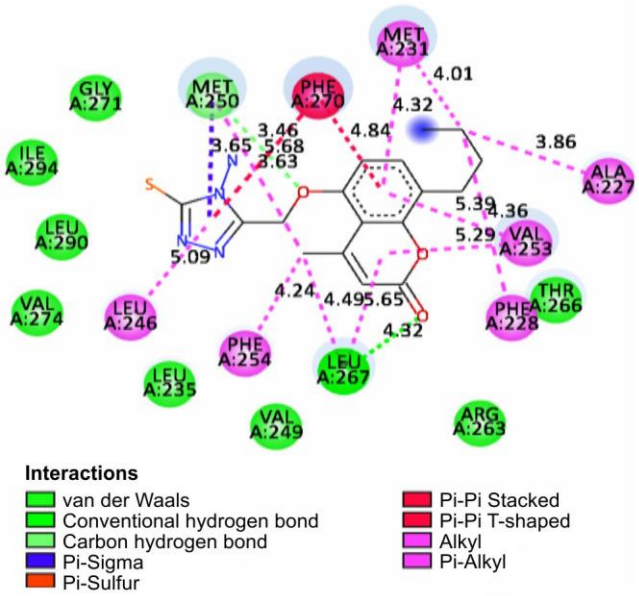
MET A:231
4.01
GLY A:271
MET A:250
PHE A:270
4.32
3.46
4.84
3.65
5.68
3.63
3.86
ALA A:227
ILE A:294
5.39
4.36
LEU A:290
5.29
VAL A:253
5.09
4.24
4.49
5.65
THR A:266
VAL A:274
LEU A:246
PHE A:228
4.32
PHE A:254
LEU A:267
LEU A:235
VAL A:249
ARG A:263
Interactions
van der Waals
Conventional hydrogen bond
Carbon hydrogen bond
Pi-Sigma
Pi-Sulfur
Pi-Pi Stacked
Pi-Pi T-shaped
Alkyl
Pi-Alkyl

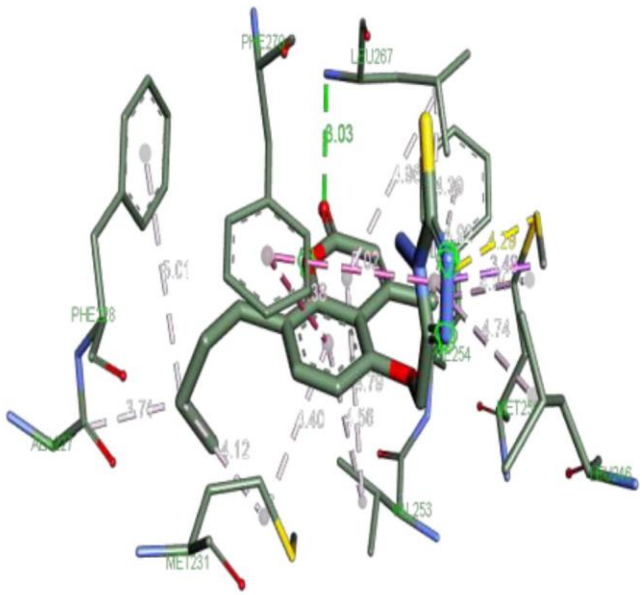

8g

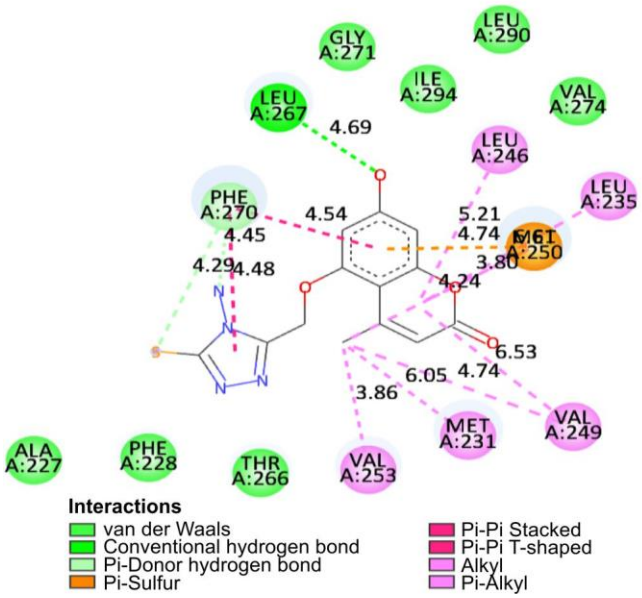
LEU A:290
GLY A:271
ILE A:294
VAL A:274
LEU A:267
4.69
LEU A:246
LEU A:235
PHE A:270
4.54
5.21
4.74
MET A:250
4.45
3.80
4.29
4.48
4.24
6.53
6.05
4.74
3.86
MET A:231
VAL A:249
ALA A:227
PHE A:228
THR A:266
VAL A:253
Interactions
van der Waals
Conventional hydrogen bond
Pi-Donor hydrogen bond
Pi-Sulfur
Pi-Pi Stacked
Pi-Pi T-shaped
Alkyl
Pi-Alkyl

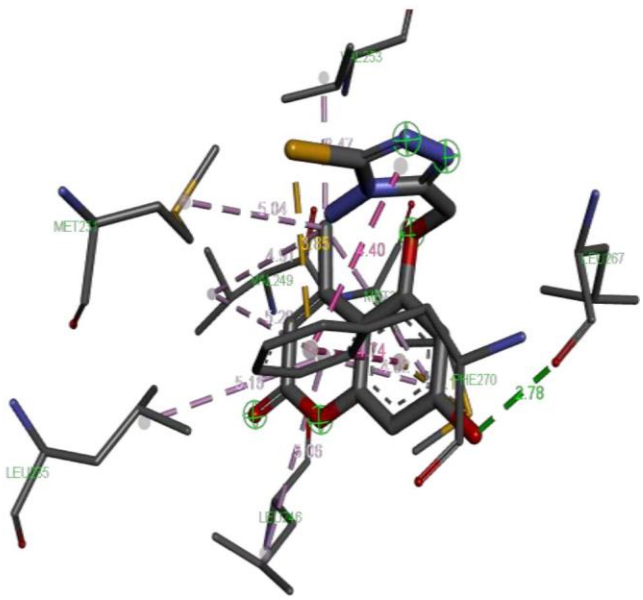

8h

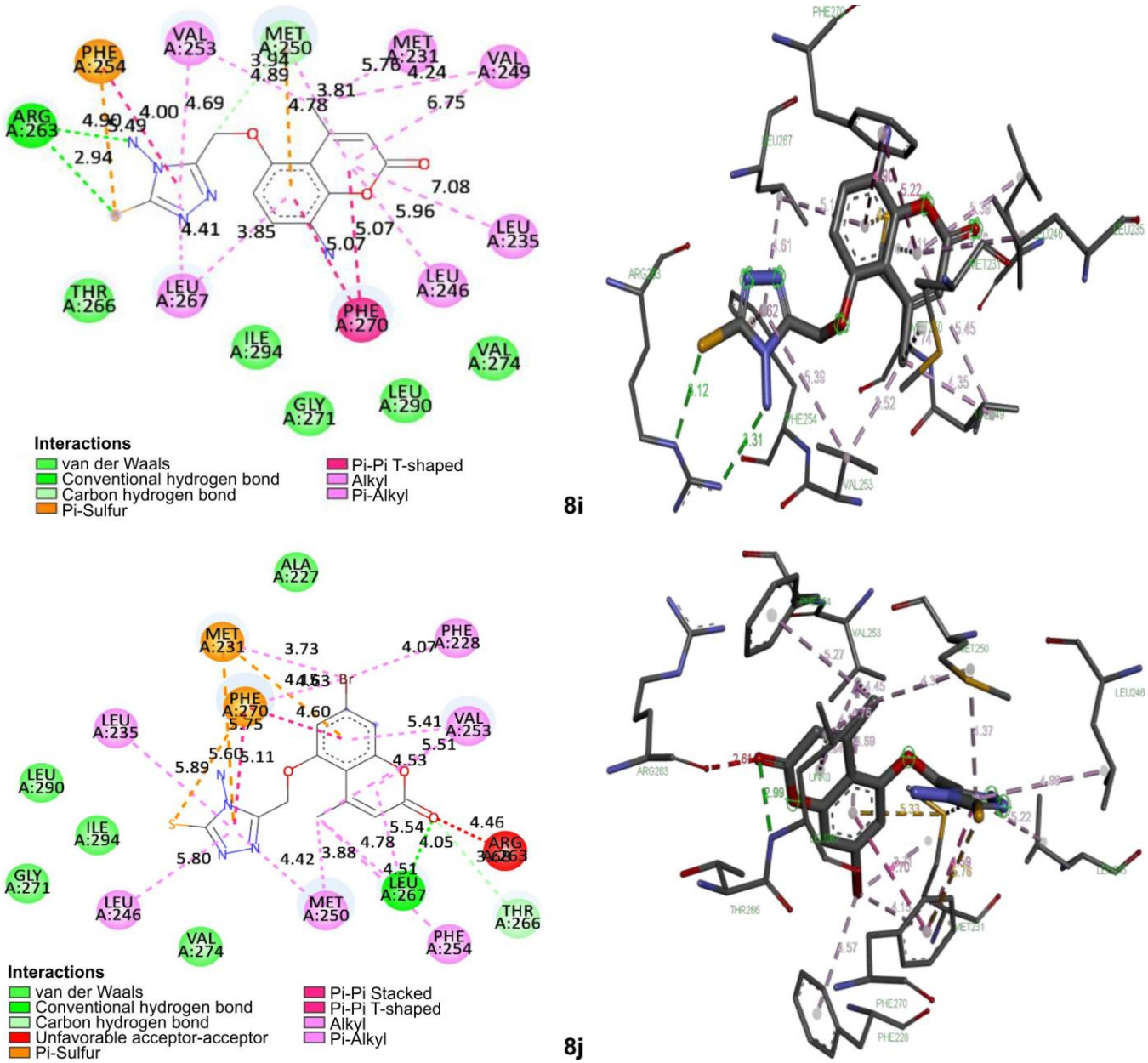

Fig. 1. 2D and 3D interactions of compounds **8a-j** at target protein 3WIX

ged as the best-performing derivative, which can be attributed to the presence of a *para*-substituted halogen group, enhancing hydrophobic and electrostatic interactions with key active site residues. This was followed by compounds **8d** and **8e**, both exhibiting docking scores of -9.92 kcal/mol, suggesting that both electron-withdrawing (–Cl) and electron-donating (-NH_2) substituents significantly contribute to improve the binding affinity.

Compounds **8b** and **8i** also showed favourable docking scores of -9.88 kcal/mol, indicating that *para*-substitution on the coumarin phenyl ring, particularly with electron-donating or moderately lipophilic groups, promotes efficient binding. Similarly, compounds **8j** and **8a** displayed good binding affinities with scores of -19.85 and -9.82 kcal/mol, respectively, suggesting that bulky alkyl and halogen substituents at the *para* position are well tolerated within the MCL-1 binding pocket.

Compounds **8f** and **8c** exhibited moderate binding affinities (-9.77 and -9.62 kcal/mol, respectively), indicating that *meta*-hydroxyl or *para*-amino substitutions provide reasonable stabilization through hydrogen bonding interactions. In contrast, compound **8g** showed the lowest docking score (-9.60 kcal/mol), likely due to steric hindrance associated with *meta*-bromine substitution, which may limit optimal interaction with the active-site residues.

Overall, the docking analysis clearly demonstrates that *para*-substituted coumarin derivatives exhibit superior binding affinity toward the MCL-1 receptor, highlighting the critical role of substitution pattern and electronic effects in modulating protein–ligand interactions. These findings support the potential of the synthesized compounds as promising MCL-1 inhibitors and provide valuable insights for further structural optimization.

Anticancer activity: The anticancer effectiveness of hybrids **8a-j** on MDA-MB-231 (breast cancer) cell lines was assessed using an MTT assay. The MDA-MB-231 cell line, a well-established triple-negative breast cancer (TNBC) model, was employed to evaluate the antiproliferative potential of the synthesized compounds using the MTT assay. This colorimetric assay measures cellular metabolic activity based on the reduction of the yellow tetrazolium salt 3-(4,5-dimethylthiazol-2-yl)-2,5-diphenyltetrazolium bromide (MTT) to insoluble purple formazan crystals by viable cells.

Following treatment, MTT solution (5 mg/mL in PBS) was added to each well and incubated to allow metabolically active cells to reduce the dye to formazan. The culture medium was subsequently removed and the formed crystals were dissolved using DMSO solvent. Absorbance was measured using a microplate reader at 570 nm, with a reference wavelength of 630 nm. Cell viability was directly proportional to the measured absorbance. All experiments were performed in triplicate (n = 3) under sterile conditions to ensure reproducibility and accuracy.

Dose-response curves were generated by plotting percentage cell viability against compound concentration, enabling the determination of IC_{50} values, defined as the concentration required to inhibit 50% of cell growth. Among the evaluated derivatives, halogen-substituted compounds exhibited enhanced antiproliferative activity. Notably, the *para*-bromo coumarin derivative **8h** showed the highest potency with an IC_{50} value of 3.30 μM, whereas the *meta*-bromo analogue **8g** displayed significantly lower activity (IC_{50} = 15.15 μM), indicating the critical influence of substitution position.

Compounds **8b**, **8i** and **8j** demonstrated strong anticancer activity with IC_{50} values of 4.36, 4.76 and 4.97 μM, respectively, while compound **8a** exhibited moderate potency (IC_{50} = 5.35 μM). Moreover, compounds **8d** and **8e** showed notable antitumor activity with IC_{50} values of 6.33 and 6.39 μM, respectively (Table-2). The enhanced activity of these derivatives may be attributed to their ability to form favourable hydrogen-bonding interactions with intracellular targets, thereby improving binding affinity and cytotoxic efficacy.

TABLE-2
INHIBITORY CONCENTRATIONS (IC_{50}) DATA OF THE SYNTHESIZED COMPOUNDS **8a-j**

Compound	IC_{50} (μM)	Compound	IC_{50} (μM)
8a	5.35	**8g**	15.15
8b	4.36	**8h**	3.30
8c	14.83	**8i**	4.76
8d	6.33	**8j**	4.97
8e	6.39	Reference	1.01
8f	12.89		

Structure–activity relationship (SAR) analysis revealed that *para*-substitution on the coumarin moiety, particularly with bromo (-Br), amino/alkyl and chloro or hydroxyl containing groups, consistently resulted in improved anticancer activity. In contrast, compounds **8f** (IC_{50} = 12.89 μM) and **8c** (IC_{50} = 14.83 μM) showed comparatively lower cytotoxicity, although they retained measurable antiproliferative effects and demonstrated binding affinity toward target proteins. Overall, the results highlight the importance of substituent type and position in modulating anticancer potency against TNBC cells and support the potential of these derivatives as promising anticancer leads.

Conclusion

A series of coumarin based mercaptotriazoles (**8a-j**) were synthesized by reacting different diol derivatives with ethylacetoacetate in the presence of Eatons reagent as solvent to form coumarin intermediates followed by series of reactions on cyclization yield final compounds. The resulting products were recrystallized with ethanol. The synthesized compounds were thoroughly characterized using ^{1}H NMR, ^{13}C NMR, FTIR and mass spectrometry, confirming their proposed molecular structures. All evaluated derivatives exhibited notable anticancer activity against the tested cell lines. Structure–activity relationship (SAR) analysis revealed that the position of substituents and their electron-donating or electron-withdrawing nature play a critical role in modulating anticancer potency. Among the series, compound **8h** demonstrated the most pronounced antineoplastic activity against the MDA-MB-231 breast cancer cell line. In addition, molecular docking studies were carried out against the MCL-1 receptor protein, providing insights into the binding interactions and supporting the experimental anticancer findings. The combined boilogical and computational results suggest that these compounds possess promising therapeutic potential. However, further investigations into their molecular mechanisms, structure optimization and *in vivo* evaluation are necessary to fully elucidate their mode of action and to advance these molecules as potent lead candidates for the treatment of breast cancer.

ACKNOWLEDGEMENTS

The authors are grateful to the Guru Nanak Institutions Technical Campus, School of Pharmacy, Ibrahimpatnam, India, for providing the support in completing the current work.

CONFLICT OF INTEREST

The authors declare that there is no conflict of interests regarding the publication of this article.

DECLARATION OF AI-ASSISTED TECHNOLOGIES

During the preparation of this manuscript, the authors used an AI-assisted tool(s) to improve the language. The authors reviewed and edited the content and take full responsibility for the published work.

REFERENCES

1. S.A. Narod, *Nat. Rev. Clin. Oncol.*, **8**, 669 (2011); https://doi.org/10.1038/nrclinonc.2011.110.
2. K.C. Oeffinger, E.T. Fontham, R. Etzioni, A. Herzig, J.S. Michaelson, Y.C.T. Shih, L.C. Walter, T.R. Church, C.R. Flowers, S.J. LaMonte, A.M.D. Wolf, C. DeSantis, J. Lortet-Tieulent, D. Manassaram-Baptiste, K. Andrews, D. Saslow, R.A. Smith, O.W. Brawley and R. Wender, *JAMA*, **314**, 1599 (2015); https://doi.org/10.1001/jama.2015.12783
3. N. Takkar, S. Kochhar, P. Garg, A.K. Pandey, U.R. Dalal and U. Handa, *J Midlife Health*, **8**, 2 (2017); https://doi.org/10.4103/jmh.JMH_26_16

4. Z.S. Deng and J. Liu, *Comput. Biol. Med.*, **34**, 495 (2004); https://doi.org/10.1016/S0010-4825(03)00086-6
5. D. Hanahan and R.A. Weinberg, *Cell*, **144**, 646 (2011); https://doi.org/10.1016/j.cell.2011.02.013
6. S. Eser, A. Schnieke, G. Schneider and D. Saur, *Br. J. Cancer*, **111**, 817 (2014); https://doi.org/10.1038/bjc.2014.215
7. H. Lu and J. Marti, *J. Phys. Chem. Lett.*, **11**, 9938 (2020); https://doi.org/10.1021/acs.jpclett.0c02809
8. A.A. Aly, A.A. Hassan, M.M. Makhlouf and S. Bräse, *Molecules*, **25**, 3036 (2020); https://doi.org/10.3390/molecules25133036
9. F. Tok and D.D. Çelik, *Turk. J. Pharm. Sci*., **22**, 349 (2025); https://doi.org/10.4274/tjps.galenos.2025.77834.a
10. S. Nayak, S.L. Gaonkar, S.S. Hakkimane, B. Swapna and N.S. Shetty, *Asian J. Chem*., **33**, 3039 (2021); https://doi.org/10.14233/ajchem.2021.23472
11. Y. Tanaka, K. Aikawa, G. Nishida, M. Homma, S. Sogabe, S. Igaki, Y. Hayano, T. Sameshima, I. Miyahisa, T. Kawamoto, M. Tawada, Y. Imai, M. Inazuka, N. Cho, Y. Imaeda and T. Ishikawa, *J. Med. Chem.*, **56**, 9635 (2013); https://doi.org/10.1021/jm401170c
12. BIOVIA, Dassault Systèmes, Discovery Studio Visualizer, version 21.1.0.20298, San Diego, CA, USA: Dassault Systèmes (2021).
13. J. Wu, X. Liu, X. Cheng, Y. Cao, D. Wang, Z. Li, C. Pannecouque, W. Xu, M. Witvrouw and E. De Clercq, *Molecules*, **12**, 2003 (2007); https://doi.org/10.3390/12082003
14. A.M. Petros, S.L. Swann, D. Song, K. Swinger, C. Park, H. Zhang, M. D. Wendt, A.R. Kunzer, A.J. Souers and C. Sun, *Bioorg. Med. Chem. Lett.*, **24**, 1484 (2014); https://doi.org/10.1016/j.bmcl.2014.02.010